

Energy Extraction from Spinning Black Holes via Relativistic Jets

Ramesh Narayan¹, Jeffrey E. McClintock¹ and Alexander Tchekhovskoy²

¹ Harvard-Smithsonian Center for Astrophysics, Harvard University, 60 Garden St, Cambridge, MA 02138, USA

² Jadwin Hall, Princeton University, Princeton, NJ 08544, USA; Center for Theoretical Science Fellow

E-mail: rnarayan@cfa.harvard.edu, jmcclintock@cfa.harvard.edu, atchekho@princeton.edu

Abstract.

It has for long been an article of faith among astrophysicists that black hole spin energy is responsible for powering the relativistic jets seen in accreting black holes. Two recent advances have strengthened the case. First, numerical general relativistic magnetohydrodynamic simulations of accreting spinning black holes show that relativistic jets form spontaneously. In at least some cases, there is unambiguous evidence that much of the jet energy comes from the black hole, not the disk. Second, spin parameters of a number of accreting stellar-mass black holes have been measured. For ballistic jets from these systems, it is found that the radio luminosity of the jet correlates with the spin of the black hole. This suggests a causal relationship between black hole spin and jet power, presumably due to a generalized Penrose process.

1. Introduction

Relativistic jets are a common feature of accreting black holes (BHs). They are found in both stellar-mass BHs and supermassive BHs, and are often very powerful. Understanding how jets form and where they obtain their enormous power is an active area of research in astrophysics.

In seminal work, Penrose [27] showed that a spinning BH has free energy that is, in principle, available to be tapped. This led to the

popular idea that the energy source behind relativistic jets might be the rotational energy of the accreting BH. A number of astrophysical scenarios have been described in which magnetic fields enable this process [29, 5, 6, 11, 12, 19, 17, 3, 36, 21]. Field lines are kept confined around the BH by an accretion disk, and the rotation of space-time near the BH twists these lines into helical magnetic springs which expand under their own pressure, accelerating any attached plasma. Energy is thereby extracted from the spinning BH and is transported out along the magnetic field, making a relativistic jet. Although this mechanism requires accretion of magnetized fluid and is thus not the same as Penrose’s original proposal¹, we will still refer to it as the “generalized Penrose process” since ultimately the energy comes from the spin of the BH.

It is not easy to prove that the generalized Penrose process is necessarily in operation in a given jet. The reason is that jets are always associated with accretion disks, and the accretion process itself releases gravitational energy, some of which might flow into the jet. Let us define a jet efficiency factor η_{jet} ,

$$\eta_{\text{jet}} = \frac{\langle L_{\text{jet}} \rangle}{\langle \dot{M}(r_{\text{H}}) \rangle c^2}, \quad (1)$$

where $\langle L_{\text{jet}} \rangle$ is the time-average (kinetic and electromagnetic) luminosity flowing out through the jet and $\langle \dot{M}(r_{\text{H}}) \rangle c^2$ is the time-average rate at which rest-mass energy flows in through the BH horizon. Many jets, both those observed and those seen in computer simulations, have values of η_{jet} quite a bit less than unity. With such a modest efficiency, the jet power could easily come from the accretion disk [4, 9, 13].

The situation has improved considerably in the last couple of years. As we show in §2, numerical simulations have now been carried out where it can be demonstrated beyond reasonable doubt that the simulated jet obtains power directly from the BH spin energy. Furthermore, as we discuss in §3, the first observational evidence for a possible correlation between jet power and BH spin has finally been obtained. The correlation appears to favor a Penrose-like process being the energy source of jets.

¹ Penrose considered a simple model in which particles on negative energy orbits fall into a spinning BH. [37] extended the analysis to discrete particle accretion in the presence of a magnetic field, which introduces additional interesting effects. We do not discuss these particle-based mechanisms, but focus purely on fluid dynamical processes within the magnetohydrodynamic (MHD) approximation. We also do not discuss an ongoing controversy on whether or not different mechanisms based on magnetized fluids differ from one another [12].

2. Computer Simulations of Black Hole Accretion and Jets

For the last decade or so, it has been possible to simulate numerically the dynamics of MHD accretion flows in the fixed Kerr metric of a spinning BH. The dynamics of the magnetized fluid are described using the general relativistic MHD (GRMHD) equations in a fixed space-time, and the simulations are carried out in 3D in order to capture the magnetorotational instability (MRI), the agency that drives accretion [1]. Radiation is usually ignored, but this is not considered a problem since jets are usually found in systems with geometrically thick accretion disks, which are radiatively inefficient. We describe here one set of numerical experiments [36, 34] which have been run using the GRMHD code HARM [8] and which are particularly relevant for understanding the connection between the generalized Penrose process and jets.

As is standard, the numerical simulations are initialized with an equilibrium gas torus orbiting in the equatorial plane of a spinning BH. The torus is initially embedded with a weak seed magnetic field, as shown in panel (a) of Figure 1. Once the simulation begins, the magnetic field strength grows as a result of the MRI [1]. This leads to MHD turbulence, which in turn drives accretion of mass and magnetic field into the BH. The mass accretion rate is given by

$$\dot{M}(r) = - \iint_{\theta, \varphi} \rho u^r dA_{\theta, \varphi}, \quad (2)$$

where the integration is over all angles on a sphere of radius r (Boyer-Lindquist or Kerr-Schild coordinates), $dA_{\theta, \varphi} = \sqrt{-g} d\theta d\varphi$ is the surface area element, ρ is the density, u^r is the contravariant radial component of 4-velocity, and g is the determinant of the metric. The sign in equation (2) is chosen such that $\dot{M} > 0$ corresponds to mass inflow. One is usually interested in the mass accretion rate at the horizon, $\dot{M}(r = r_{\text{H}})$. In computing $\dot{M}(r_{\text{H}})$ from simulations, one waits until the system has reached approximate steady state. One then computes $\dot{M}(r_{\text{H}})$ over a sequence of many snapshots in time and then averages to eliminate turbulent fluctuations. This gives the time-average mass accretion rate $\langle \dot{M}(r_{\text{H}}) \rangle$.

Panels (b)-(d) in Figure 1 show the time evolution of the accretion flow and jet in a simulation with BH spin $a_* \equiv a/M = 0.99$, where M is the BH mass [36]. The steady accretion of magnetized fluid causes magnetic field to accumulate in the inner regions near the BH. After a while, the field becomes so strong that it compresses the inner part of the otherwise geometrically thick accretion flow into a thin sheet (panel b). The effect is to obstruct the accretion flow (panels c and d), leading to what is known as a magnetically-arrested disk [23, 10] or a magnetically choked accretion flow [20]. The strong field extracts BH spin energy and forms a powerful

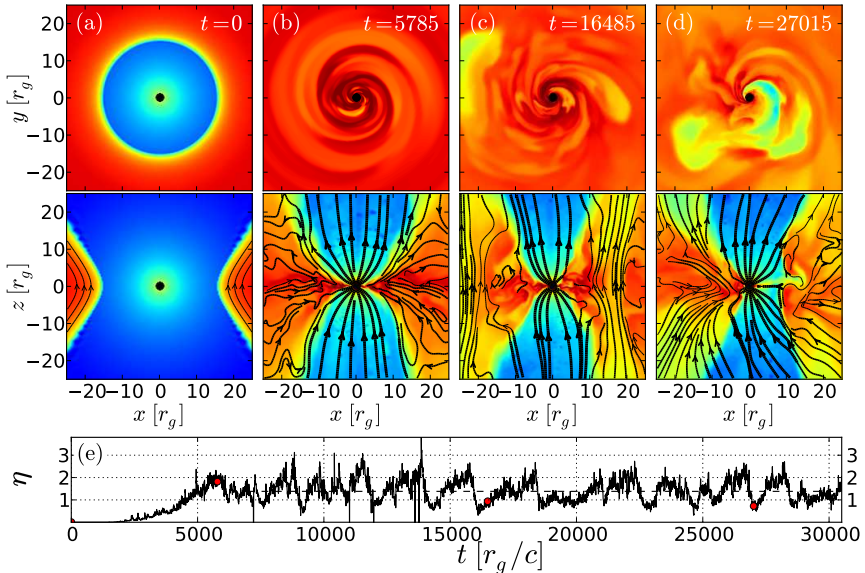


Figure 1. Formation of a magnetically-arrested disk and ejection of powerful jets in a GRMHD simulation of magnetized accretion on to a rapidly spinning BH with $a_* = 0.99$ [36]. The top and bottom rows in panels (a)-(d) show a time sequence of equatorial and meridional slices through the accretion flow. Solid lines show magnetic field lines in the image plane, and color shows $\log \rho$ (red high, blue low). The simulation starts with an equilibrium torus embedded with a weak magnetic field (panel a). The weakly magnetized orbiting gas is unstable to the MRI, which causes gas and field to accrete. As large-scale magnetic flux accumulates at the center, a coherent bundle of field lines forms at the center, which threads the BH and has the configuration of bipolar funnels along the (vertical) BH rotation axis. These funnels contain strong field and low mass density (lower panels b, c, d). Helical twisting of the field lines as a result of dragging of frames causes a powerful outflow of energy through the funnels in the form of twin jets. The outflow efficiency η (panel e), calculated as in equation (5), becomes greater than unity once the flow achieves quasi-steady state at time $t \gtrsim 5000 r_g/c$. This is the key result of the simulation. Having a time-average $\eta > 1$ means that there is a net energy flow *out* of the BH, i.e., spin energy is extracted from the BH by the magnetized accretion flow. This constitutes a demonstration of the generalized Penrose process in the astrophysically relevant context of a magnetized accretion flow.

outflow. To understand the energetics, consider the rate of flow of energy,

$$\dot{E}(r) = \iint_{\theta, \varphi} T_t^r dA_{\theta, \varphi}, \quad (3)$$

where the stress-energy tensor of the magnetized fluid is

$$T_\nu^\mu = \left(\rho + u_g + p_g + \frac{b^2}{4\pi} \right) u^\mu u_\nu + \left(p + \frac{b^2}{8\pi} \right) \delta_\nu^\mu - \frac{b^\mu b_\nu}{4\pi}, \quad (4)$$

u_g and p_g are the internal energy and pressure of the gas, b^μ is the fluid-frame magnetic field 4-vector (see [8] for the definition), and $b^2 = b^\mu b_\mu$ is the square of the fluid-frame magnetic field strength. The sign of equation (3) is chosen such that $\dot{E}(r) > 0$ corresponds to energy inflow. Note that T_t^r includes the inflow of rest mass energy via the term $\rho u^r u_t$.

Let us define the efficiency with which the accreting BH produces outflowing energy as

$$\eta = \frac{\dot{M}(r_H)c^2 - \dot{E}(r_H)}{\langle \dot{M}(r_H) \rangle c^2}, \quad (5)$$

where we have made η dimensionless by normalizing the right-hand side by the time-average mass energy accretion rate. To understand the meaning of equation (5), consider the simple example of gas falling in radially from infinity, with no radiative or other energy losses along the way. In this case, we have $\dot{E}(r_H) = \dot{M}(r_H)c^2$, i.e., the gas carries an energy equal to its rest mass energy into the BH. Hence $\eta = 0$, as appropriate for this example. For a more realistic accretion flow, some energy is lost by the gas via radiation, winds and jets, and one generally expects the energy flowing into the BH to be less than the rest mass energy: $\dot{E}(r_H) < \dot{M}(r_H)c^2$. This will result in an efficiency $\eta > 0$, where η measures the ratio of the energy returned to infinity, $\dot{M}(r_H)c^2 - \dot{E}(r_H)$, to the energetic price paid in the form of rest mass energy flowing into the BH, $\dot{M}(r_H)c^2$.

Usually, $\dot{E}(r_H)$ is positive, i.e., there is a net flow of energy into the BH through the horizon, and $\eta < 1$. However, there is no theorem that requires this. Penrose's [27] great insight was to realize that it is possible to have $\dot{E}(r_H) < 0$ (net *outward* energy flow as measured at the horizon), and thus $\eta > 1$. In the context of an accretion flow, $\dot{E}(r_H) < 0$ means that, even though rest mass flows steadily into the BH, there is a net energy flow out of the BH. As a result, the gravitational mass of the BH decreases with time. It is the energy associated with this decreasing mass that enables η to exceed unity. Of course, as the BH loses gravitational mass, it also loses angular momentum and spins down. This can be verified by considering the angular momentum flux at the horizon, $\dot{J}(r_H)$, which may be computed as in equation (3) but with T_t^r replaced by T_ϕ^r (e.g., [26]).

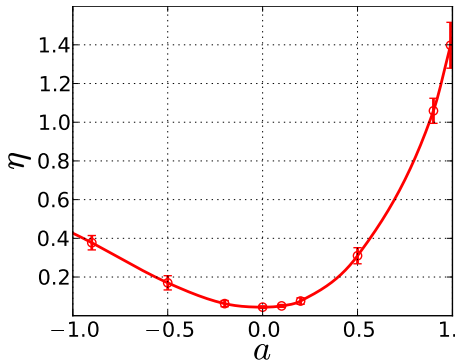


Figure 2. Time-average outflow efficiency η versus BH spin parameter a_* for a sequence of GRMHD simulations of non-radiative BH accretion flows [34]. The efficiency exceeds unity for $a_* \gtrsim 0.9$. Negative values of a_* correspond to the accretion flow counter-rotating with respect to the BH.

Returning to the simulation under consideration, Figure 1(e) shows the outflow efficiency η as a function of time. It is seen that the average efficiency exceeds unity once the flow achieves steady state at time $t \gtrsim 5000r_g/c$, where $r_g = GM/c^2$. The outflow thus carries away more energy than the entire rest mass energy brought in by the accretion flow. This is an unambiguous demonstration of the generalized Penrose process in the astrophysically plausible setting of a magnetized accretion flow on to a spinning BH. Of course, it is not obvious that the energy necessarily flows out in a collimated relativistic jet, since the quantity η is defined via global integrals (eqs. 2, 5) which do not specify exactly where the outflowing energy ends up. A more detailed analysis reveals that the bulk of the energy does indeed go into a relativistic jet, while about 10% goes into a quasi-relativistic wind [34].

Figure 1 corresponds to an extreme example, viz., a very rapidly spinning BH with $a_* = 0.99$. Figure 2 shows results from a parameter study that investigated the effect of varying a_* . It is seen that the time-average η increases steeply with increasing a_* . For an accretion flow that corotates with the BH, the power going into the jet can be well-fit with a power-law dependence,

$$\eta_{\text{jet}} \approx 0.65a_*^2(1 + 0.85a_*^2). \quad (6)$$

This approximation remains accurate to within 15% for $0.3 \leq a_* \leq 1$. For low spins, the net efficiency derived from the simulations is greater than that predicted by equation (6). For example, as Figure 2 shows, the simulation gives a non-zero value of η for $a_* = 0$, which is inconsistent

with equation (6). This is because, for $a_* = 0$, all the outflow energy comes directly from the accretion flow, most of which goes into a wind. Nothing comes from the BH, whereas equation (6) refers specifically to the efficiency η_{jet} associated with jet power from the BH. With increasing BH spin, both the disk and the hole contribute to energy outflow, with the latter becoming more and more dominant. For spin values $a_* > 0.9$, the BH’s contribution is so large that the net efficiency exceeds unity.

Before leaving this topic, we note that other numerical simulations have used geometrically thicker accretion configurations than the one shown in Figure 1 and find even larger values of η [33, 20].

3. Empirical Evidence for the Generalized Penrose Process

As discussed in §2, there is definite evidence from computer simulations that the generalized Penrose process is feasible, and even quite plausible, with magnetized accretion flows. We discuss here recent progress on the observational front. In §3.1 we briefly summarize efforts to measure spin parameters of astrophysical BHs. Then in §3.2 we discuss a correlation that has been found between jet power and BH spin. Finally in §3.3 we explain why we think the observational evidence favors a Penrose-like process rather than disk power.

3.1. Spin Parameters of Stellar-Mass Black Holes

In 1989, the first practical approach to measuring black hole spin was suggested [7], viz., modeling the relativistically-broadened Fe K emission line emitted from the inner regions of an accretion disk. The first compelling observation of such a line was reported six years later [32]. Presently, the spins of more than a dozen black holes have been estimated by modeling the Fe K line (see [28] for a recent review).

In 1997, a second approach to measuring black hole spin, the “continuum-fitting method,” was proposed [38]. In this method, one fits the thermal continuum spectrum of a black hole’s accretion disk to the relativistic model of Novikov & Thorne [25]. One then identifies the inner edge of the modeled disk with the radius R_{ISCO} of the innermost stable circular orbit (ISCO) in the space-time metric. Since R_{ISCO} varies monotonically with respect to the dimensionless BH spin parameter a_* (see Fig. 3), a measurement of the former immediately provides an estimate of the latter.

In 2006, the continuum-fitting method was employed to estimate the spins of three stellar-mass BHs [30, 15]. Seven additional spins have since been measured. Table 1 lists the masses and spins of these ten BHs. Readers are referred to a recent review [14] for details of the continuum-fitting method and uncertainties in the derived spin estimates.

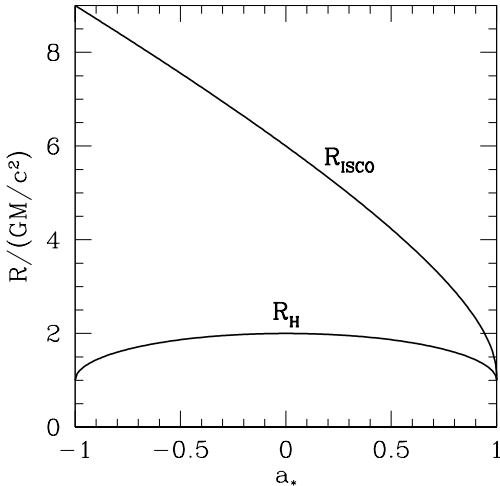


Figure 3. Radius of the ISCO R_{ISCO} and of the horizon R_{H} in units of GM/c^2 plotted as a function of the black hole spin parameter a_* . Negative values of a_* correspond to retrograde orbits. Note that R_{ISCO} decreases monotonically from $9GM/c^2$ for a retrograde orbit around a maximally spinning black hole, to $6GM/c^2$ for a non-spinning black hole, to GM/c^2 for a prograde orbit around a maximally spinning black hole.

The continuum-fitting method is simple and demonstrably robust. It does not make many assumptions; those few it makes have nearly all been tested and shown to be valid (see [16, 14] for details). A significant limitation of the method is that it is only readily applicable to stellar-mass BHs. For such BHs, however, we would argue that it is the method of choice. The Fe K method can be applied to both stellar-mass and supermassive BHs. For the latter, it is the only method currently available.

3.2. Correlation Between Black Hole Spin and Jet Radio Power

The 10 stellar-mass BHs in Table 1 are divided into two classes: “persistent” sources, which are perennially bright in X-rays at a relatively constant level, and “transient” sources, which have extremely large amplitude outbursts. During outburst, the transient sources generally reach close to the Eddington luminosity limit (see [31] for a quantitative discussion of this point). Close to the peak, these systems eject blobs of plasma that move ballistically outward at relativistic speeds (Lorentz

Table 1. The spins and masses of ten stellar-mass black holes [14].

System	a_*	M/M_\odot
Persistent		
Cygnus X-1	> 0.95	14.8 ± 1.0
LMC X-1	$0.92^{+0.05}_{-0.07}$	10.9 ± 1.4
M33 X-7	0.84 ± 0.05	15.65 ± 1.45
Transient		
GRS 1915+105	> 0.95	10.1 ± 0.6
4U 1543-47	0.80 ± 0.10	9.4 ± 1.0
GRO J1655-40	0.70 ± 0.10	6.3 ± 0.5
XTE J1550-564	0.34 ± 0.24	9.1 ± 0.6
H1743-322	0.2 ± 0.3	~ 8
LMC X-3	< 0.3	7.6 ± 1.6
A0620-00	0.12 ± 0.19	6.6 ± 0.25

factor $\Gamma > 2$). These ballistic jets are often visible in radio and sometimes in X-rays out to distances of order a parsec from the BH, i.e., to distances $> 10^{10}GM/c^2$. Because ballistic jets resemble the kiloparsec-scale jets seen in quasars, stellar-mass BHs that produce them are called microquasars [22].

On general principles, one expects the jet luminosity L_{jet} (the power flowing out in the kinetic and electromagnetic energy) to depend on the BH mass M , its spin a_* , and the mass accretion rate \dot{M} (plus perhaps other qualitative factors such as the topology of the magnetic field [2, 18]). If one wishes to investigate the dependence of jet luminosity on a_* , one needs first to eliminate the other two variables. Ballistic jets from transient stellar-mass BHs are very well-suited for this purpose. First, the BH masses are similar to better than a factor of two (see Table 1). Second, all these sources have similar accretion rates, close to the Eddington limit, at the time they eject their ballistic jets [31]. This leaves a_* as the only remaining variable.

Narayan & McClintock [24] considered the peak radio luminosities of ballistic jet blobs in four transient BHs, A0620-00, XTE J1550-564, GRO J1655-40, GRS 1915+105, and showed that they correlate well with the corresponding black hole spins measured via the continuum-fitting

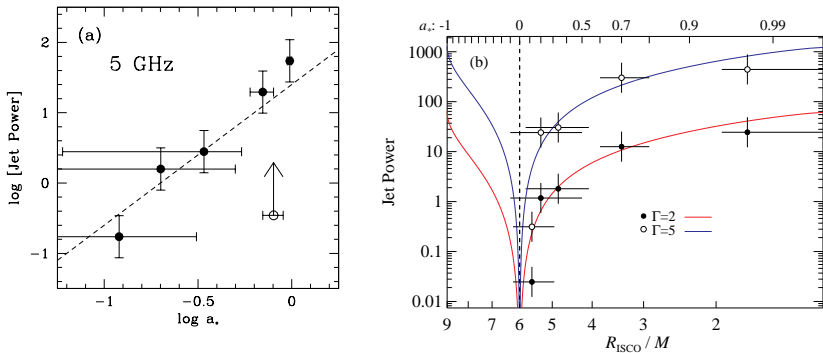


Figure 4. (a) Plot of jet power estimated from 5 GHz radio flux at light curve maximum, versus black hole spin measured via the continuum-fitting method, for five transient stellar-mass BHs [24, 31]. The dashed line has slope fixed to 2 (see eq. 6) and is not a fit. (b) Plot of jet power versus $R_{\text{ISCO}}/(GM/c^2)$. Here jet power has been corrected for beaming assuming jet Lorentz factor $\Gamma = 2$ (filled circles) or $\Gamma = 5$ (open circles). The two solid lines correspond to fits of a relation of the form, “Jet Power” $\propto \Omega_{\text{H}}^2$, where Ω_{H} is the angular frequency of the black hole horizon [31]. Note that jet power varies by a factor $\gtrsim 1000$ among the five objects shown.

method². Later, [31] included a fifth BH, H1743-322, whose spin had been just measured. Figure 4a shows the inferred ballistic jet luminosities of these five objects plotted versus black hole spin. The quantity “Jet Power” along the vertical axis refers to the scaled maximum radio luminosity $(\nu S_\nu)D^2/M$, where ν ($= 5$ GHz) is the radio frequency at which the measurements are made, S_ν is the radio flux density in janskys at this frequency at the peak of the ballistic jet radio light curve, D is the distance in kiloparsecs, and M is the black hole mass in solar units. There is unmistakable evidence for a correlation between the observationally determined quantity Jet Power and a_* . Although there are only five data points, note that Jet Power varies by nearly three orders of magnitude as the spin parameter varies from $\approx 0.1 - 1$.

The very unequal horizontal errorbars in Figure 4a are a feature of the continuum-fitting method of measuring a_* . Recall that the method in effect measures R_{ISCO} and then deduces the value of a_* using the mapping

² In the case of a fifth transient BH, 4U1543-47, radio observations did not include the peak of the light curve, so one could only deduce a lower limit to the jet power, which is shown as an open circle in Figure 4a.

shown in Figure 3. Since the mapping is non-linear, especially as $a_* \rightarrow 1$, comparable errors in R_{ISCO} correspond to very different uncertainties in a_* . In addition, the use of $\log a_*$ along the horizontal axis tends to stretch errorbars excessively for low spin values. Figure 4b, based on [31], illustrates these effects. Here the horizontal axis tracks $\log R_{\text{ISCO}}$ rather than $\log a_*$, and the horizontal errorbars are therefore more nearly equal. The key point is, regardless of how one plots the data, the correlation between Jet Power and black hole spin appears to be strong.

3.3. Why Generalized Penrose Process?

Assuming the correlation shown in Figure 4 is real, there are two immediate implications: (i) Ballistic jets in stellar-mass BHs are highly sensitive to the spins of their underlying BHs. (ii) Spin estimates of stellar-mass BHs obtained via the continuum-fitting method are sufficiently reliable to reveal this long-sought connection between relativistic jets and BH spin.

With respect to (i), the mere existence of a correlation does not necessarily imply that the generalized Penrose process is at work. We know that the accretion disk itself is capable of producing a jet-like outflow [4, 9, 13]. Furthermore, the gravitational potential well into which an accretion disk falls becomes deeper with increasing BH spin, since the inner radius of the disk R_{ISCO} becomes smaller (Fig. 3). Therefore, a disk-driven jet is likely to become more powerful with increasing spin. Could this be the reason for the correlation between Jet Power and spin seen in Figure 4? We consider it unlikely. The radiative efficiency η_{disk} of a Novikov-Thorne thin accretion disk increases only modestly with spin; for the spins of the five objects shown in Figure 4, $\eta_{\text{disk}} = 0.061, 0.069, 0.072, 0.10$ and 0.19 , respectively, varying by only a factor of three. Of course, there is no reason why the power of a disk-driven jet should necessarily scale like η_{disk} . Nevertheless, the fact that η_{disk} shows only a factor of three variation makes it implausible that a disk-powered jet could have its radio luminosity vary by three orders of magnitude.

In contrast, any mechanism that taps directly into the BH spin energy via some kind of generalized Penrose process can easily account for the observed variation in Jet Power. Analytical models of magnetized accretion predict that the jet efficiency factor should vary as $\eta_{\text{jet}} \propto a_*^2$ [29, 5] or $\eta_{\text{jet}} \propto \Omega_{\text{H}}^2$ [35], where Ω_{H} is the angular frequency of the BH horizon³. The dashed line in Figure 4a corresponds to the former scaling, and the solid lines in Figure 4b to the latter scaling; equation (6), which is obtained by fitting simulation results, is intermediate between the two. The observational data agree remarkably well with the predicted scalings, strongly suggesting that the generalized Penrose process is in operation.

³ The two scalings agree for small values of a_* , but differ as $a_* \rightarrow 1$.

We cannot tell whether the energy extraction in the observed systems is mediated specifically by magnetic fields (as in the simulations), since there is no way to observe what is going on near the BH at the place where the jet is initially launched. Where the ballistic jet blobs are finally observed they are clearly magnetized — it is what enables the charged particles to produce radiation via the synchrotron mechanism — but this is at distances $\sim 10^{10}GM/c^2$.

4. Summary

In summary, the case for a generalized version of the Penrose process being the power source behind astrophysical jets has become significantly stronger in the last few years. Computer simulations have been very helpful in this regard since they enable one to study semi-realistic configurations of magnetized accretion flows and to explore quantitatively how mass, energy and angular momentum flow through the system. Recent computer experiments find unambiguous indications for energy extraction from spinning BHs via magnetic fields. Whether these simulated models describe real BHs in nature is not yet certain. However, completely independent observational data suggest a link between the spins of transient stellar-mass BHs and the energy output in ballistic jets ejected from these systems. The observationally measured quantity “Jet Power” in Figure 4 increases steeply with the measured BH spin, and the dependence is quite similar to that found both in simple analytical models [29, 5] and in simulations (Fig. 2). Taking all the evidence into account, the authors believe that Penrose’s seminal ideas on energy extraction from spinning BHs are relevant for the production of at least some categories of relativistic astrophysical jets.

The authors thank J. F. Steiner for help with Fig. 4b. RN’s work was supported in part by NASA grant NNX11AE16G. AT was supported by a Princeton Center for Theoretical Science fellowship and an XSEDE allocation TG-AST100040 on NICS Kraken and Nautilus and TACC Ranch.

References

- [1] Balbus, S. A. and Hawley, J. F., “Instability, turbulence, and enhanced transport in accretion disks”, *Reviews of Modern Physics*, **70**, 1–53, (January 1998).
- [2] Beckwith, K., Hawley, J. F. and Krolik, J. H., “The Influence of Magnetic Field Geometry on the Evolution of Black Hole Accretion Flows: Similar Disks, Drastically Different Jets”, *ApJ*, **678**, 1180–1199, (May 2008).

- [3] Beskin, V. S., *MHD Flows in Compact Astrophysical Objects: Accretion, Winds and Jets*, ISBN 978-3-642-01289-1. Springer-Verlag Berlin Heidelberg, (2010).
- [4] Blandford, R. D. and Payne, D. G., “Hydromagnetic flows from accretion discs and the production of radio jets”, *MNRAS*, **199**, 883–903, (June 1982).
- [5] Blandford, R. D. and Znajek, R. L., “Electromagnetic extraction of energy from Kerr black holes”, *MNRAS*, **179**, 433–456, (May 1977).
- [6] Damour, T., Ruffini, R., Hanni, R. S. and Wilson, J. R., “Regions of magnetic support of a plasma around a black hole”, *Phys. Rev. D*, **17**, 1518–1523, (March 1978).
- [7] Fabian, A. C., Rees, M. J., Stella, L. and White, N. E., “X-ray fluorescence from the inner disc in Cygnus X-1”, *MNRAS*, **238**, 729–736, (May 1989).
- [8] Gammie, C. F., McKinney, J. C. and Tóth, G., “HARM: A Numerical Scheme for General Relativistic Magnetohydrodynamics”, *ApJ*, **589**, 444–457, (May 2003).
- [9] Ghosh, P. and Abramowicz, M. A., “Electromagnetic extraction of rotational energy from disc-fed black holes - The strength of the Blandford-Znajek process”, *MNRAS*, **292**, 887, (December 1997).
- [10] Igumenshchev, I. V., “Magnetically Arrested Disks and the Origin of Poynting Jets: A Numerical Study”, *ApJ*, **677**, 317–326, (April 2008).
- [11] Koide, S., Shibata, K., Kudoh, T. and Meier, D. L., “Extraction of Black Hole Rotational Energy by a Magnetic Field and the Formation of Relativistic Jets”, *Science*, **295**, 1688–1691, (March 2002).
- [12] Komissarov, S. S., “Blandford-Znajek Mechanism versus Penrose Process”, *J. Korean Phys. Soc.*, **54**, 2503, (June 2009).
- [13] Livio, M., Ogilvie, G. I. and Pringle, J. E., “Extracting Energy from Black Holes: The Relative Importance of the Blandford-Znajek Mechanism”, *ApJ*, **512**, 100–104, (February 1999).
- [14] McClintock, J. E., Narayan, R. and Steiner, J. F., “Black Hole Spin via Continuum Fitting and the Role of Spin in Powering Transient Jets”, *Proc. ISSI-Bern Workshop on “The Physics of Accretion onto Black Holes”*, *Space Sci. Rev. and Space Sci. Series of ISSI*, eds. T Belloni, P. Casella, M. Falanga, M. Gilfanov, P. Jonker, A. King, in press (2013, *arXiv/astro-ph:1303.1583*).
- [15] McClintock, J. E., Shafee, R., Narayan, R., Remillard, R. A., Davis, S. W. and Li, L.-X., “The Spin of the Near-Extreme Kerr Black Hole GRS 1915+105”, *ApJ*, **652**, 518–539, (November 2006).
- [16] McClintock, J. E. et al., “Measuring the spins of accreting black holes”, *CQG*, **28**(11), 114009, (June 2011).
- [17] McKinney, J. C., “General relativistic magnetohydrodynamic simulations of the jet formation and large-scale propagation from black hole accretion systems”, *MNRAS*, **368**, 1561–1582, (June 2006).
- [18] McKinney, J. C. and Blandford, R. D., “Stability of relativistic jets from rotating, accreting black holes via fully three-dimensional magnetohydrodynamic simulations”, *MNRAS*, **394**, L126–L130, (March 2009).

- [19] McKinney, J. C. and Gammie, C. F., “A Measurement of the Electromagnetic Luminosity of a Kerr Black Hole”, *ApJ*, **611**, 977–995, (August 2004).
- [20] McKinney, J. C., Tchekhovskoy, A. and Blandford, R. D., “General relativistic magnetohydrodynamic simulations of magnetically choked accretion flows around black holes”, *MNRAS*, **423**, 3083–3117, (July 2012).
- [21] Meier, D. L., *Black Hole Astrophysics: The Engine Paradigm*, by David L. Meier. ISBN: 978-3-642-01935-7. Springer-Verlag Berlin Heidelberg, (2012).
- [22] Mirabel, I. F. and Rodríguez, L. F., “Sources of Relativistic Jets in the Galaxy”, *ARAA*, **37**, 409–443, (1999).
- [23] Narayan, R., Igumenshchev, I. V. and Abramowicz, M. A., “Magnetically Arrested Disk: an Energetically Efficient Accretion Flow”, *PASJ*, **55**, L69–L72, (December 2003).
- [24] Narayan, R. and McClintock, J. E., “Observational evidence for a correlation between jet power and black hole spin”, *MNRAS*, **419**, L69–L73, (January 2012).
- [25] Novikov, I. D. and Thorne, K. S., “Astrophysics of black holes.”, in Dewitt, C. and Dewitt, B. S., eds., *Black Holes (Les Astres Occlus)*, pp. 343–450, (1973).
- [26] Penna, R. F., McKinney, J. C., Narayan, R., Tchekhovskoy, A., Shafee, R. and McClintock, J. E., “Simulations of magnetized discs around black holes: effects of black hole spin, disc thickness and magnetic field geometry”, *MNRAS*, **408**, 752–782, (October 2010).
- [27] Penrose, R., “Gravitational Collapse: the Role of General Relativity”, *Nuovo Cimento Rivista Serie*, **1**, 252, (1969).
- [28] Reynolds, C. S., “Measuring Black Hole Spin using X-ray Reflection Spectroscopy”, *Proc. ISSI-Bern Workshop on “The Physics of Accretion onto Black Holes”*, *Space Sci. Rev. and Space Sci. Series of ISSI*, eds. T Belloni, P. Casella, M. Falanga, M. Gilfanov, P. Jonker, A. King, in press (2013, [arXiv/astro-ph:1302.3260](https://arxiv.org/abs/1302.3260)).
- [29] Ruffini, R. and Wilson, J. R., “Relativistic magnetohydrodynamical effects of plasma accreting into a black hole”, *Phys. Rev. D*, **12**, 2959–2962, (November 1975).
- [30] Shafee, R., McClintock, J. E., Narayan, R., Davis, S. W., Li, L.-X. and Remillard, R. A., “Estimating the Spin of Stellar-Mass Black Holes by Spectral Fitting of the X-Ray Continuum”, *ApJL*, **636**, L113–L116, (January 2006).
- [31] Steiner, J. F., McClintock, J. E. and Narayan, R., “Jet Power and Black Hole Spin: Testing an Empirical Relationship and Using it to Predict the Spins of Six Black Holes”, *ApJ*, **762**, 104, (January 2013).
- [32] Tanaka, Y. et al., “Gravitationally redshifted emission implying an accretion disk and massive black hole in the active galaxy MCG-6-30-15”, *Nature*, **375**, 659–661, (June 1995).
- [33] Tchekhovskoy, A. and McKinney, J. C., “Prograde and retrograde black holes: whose jet is more powerful?”, *MNRAS*, **423**, L55–L59, (June

- 2012).
- [34] Tchekhovskoy, A., McKinney, J. C. and Narayan, R., “General Relativistic Modeling of Magnetized Jets from Accreting Black Holes”, *Journal of Physics Conference Series*, **372**(1), 012040, (July 2012).
 - [35] Tchekhovskoy, A., Narayan, R. and McKinney, J. C., “Black Hole Spin and The Radio Loud/Quiet Dichotomy of Active Galactic Nuclei”, *ApJ*, **711**, 50–63, (March 2010).
 - [36] Tchekhovskoy, A., Narayan, R. and McKinney, J. C., “Efficient generation of jets from magnetically arrested accretion on a rapidly spinning black hole”, *MNRAS*, **418**, L79–L83, (November 2011).
 - [37] Wagh, S. M. and Dadhich, N., “The energetics of black holes in electromagnetic fields by the penrose process”, *Phys. Rept.*, **183**, 137–192, (November 1989).
 - [38] Zhang, S. N., Cui, W. and Chen, W., “Black Hole Spin in X-Ray Binaries: Observational Consequences”, *ApJL*, **482**, L155, (June 1997).